Electronic Supplementary Information

Highly sensitive turn-on ratiometric luminescent probe based on postsynthetic modification Tb^{3+}@Cu-MOF for H_2S detection

Xubin Zheng,[a] Ruiqing Fan,*[a] Yang Song,[a] Ani Wang,[a] Kai Xing,[a] Xi Du,[a] Ping Wang[a] and Yulin Yang*[a]

[a] MIIT Key Laboratory of Critical Materials Technology for New Energy Conversion and Storage, School of Chemistry and Chemical Engineering, Harbin Institute of Technology, P. R. China *E-mail: fanruiqing@hit.edu.cn; ylyang@hit.edu.cn

Table S1. Selected bond lengths (Å) and bond angles (°) for MOFs **Cu1** and **Cu2**.

Cu1			
Cu(1)-O(2)	1.959(3)	O(2)-Cu(1)-O(2)#1	180.0
Cu(1)-N(1)	2.020(3)	O(2)-Cu(1)-N(1)#1	90.89(13)
		O(2)-Cu(1)-N(1)	89.11(13)
Cu2			
Cu(1)-O(2)	1.916(4)	N(1)-Cu(1)-O(9)#2	82.33(15)
Cu(1)-N(1)	2.154(5)	O(2)-Cu(1)-O(9)#3	88.56(15)
Cu(1)-O(9)#2	2.665(5)	N(1)-Cu(1)-O(9)#3	97.67(15)
Cu(2)-O(10)	1.886(4)	O(9)#2-Cu(1)-O(9)#3	180.0
Cu(2)-O(8)	1.940(4)	O(10)-Cu(2)-O(8)	95.14(17)
Cu(2)-O(6)#4	1.994(4)	O(10)-Cu(2)-O(6)#4	91.28(16)
Cu(2)-N(2)	2.002(5)	O(8)-Cu(2)-O(6)#4	173.27(16)
Cu(2)-O(3)#5	2.445(4)	O(10)-Cu(2)-N(2)	171.73(19)
Cu(3)-O(10)#7	1.893(4)	O(8)-Cu(2)-N(2)	87.28(18)
Cu(3)-O(9)	1.959(4)	O(6)#4-Cu(2)-N(2)	86.08(17)
Cu(3)-O(5)#8	1.973(4)	O(10)-Cu(2)-O(3)#5	98.56(16)
Cu(3)-O(4)	1.979(4)	O(4)-Cu(3)-O(4)#9	82.72(17)
Cu(3)-O(4)#9	2.584(5)	O(8)-Cu(2)-O(3)#5	93.04(18)
		O(6)#4-Cu(2)-O(3)#5	87.98(16)
O(2)-Cu(1)-O(2)#1	180.000(1)	N(2)-Cu(2)-O(3)#5	89.19(17)
O(2)-Cu(1)-N(1)	88.16(16)	O(10)#7-Cu(3)-O(9)	155.2(2)
O(2)#1-Cu(1)-N(1)	91.84(16)	O(10)#7-Cu(3)-O(5)#8	96.98(17)
N(1)#1-Cu(1)-N(1)	179.999(2)	O(9)-Cu(3)-O(5)#8	88.76(16)
O(10)#7-Cu(3)-O(4)	85.80(17)	O(10)#7-Cu(3)-O(4)#9	105.18(16)
O(9)-Cu(3)-O(4)	93.04(17)	O(9)-Cu(3)-O(4)#9	99.24(17)
O(5)#8-Cu(3)-O(4)	169.24(19)	O(5)#8-Cu(3)-O(4)#9	86.52(15)
O(2)-Cu(1)-O(9)#2	91.44(15)		

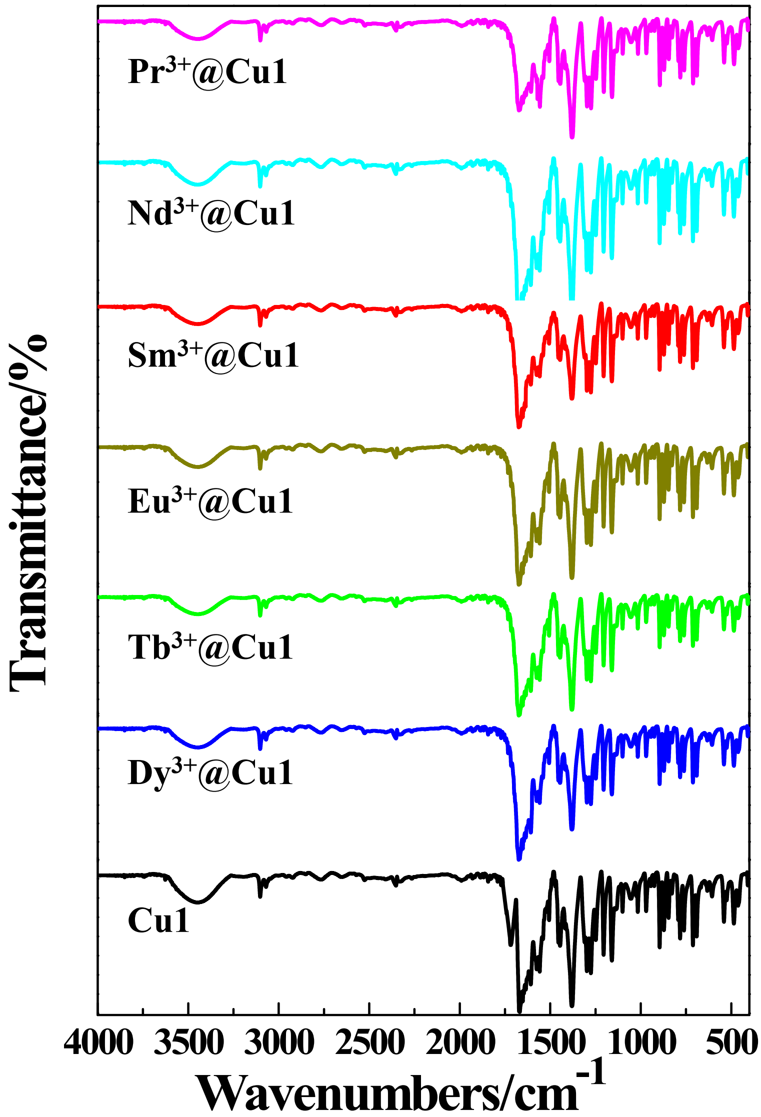

Fig. S1 The IR spectra of **Ln^{3+}@Cu1** (Ln^{3+} = Pr^{3+}, Nd^{3+}, Sm^{3+}, Eu^{3+}, Tb^{3+} and Dy^{3+}) and **Cu1**.

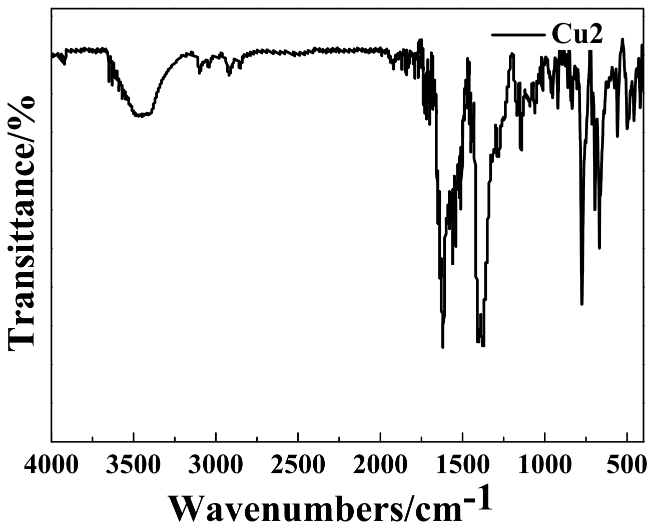

Fig. S2 The IR spectra of **Cu2.**

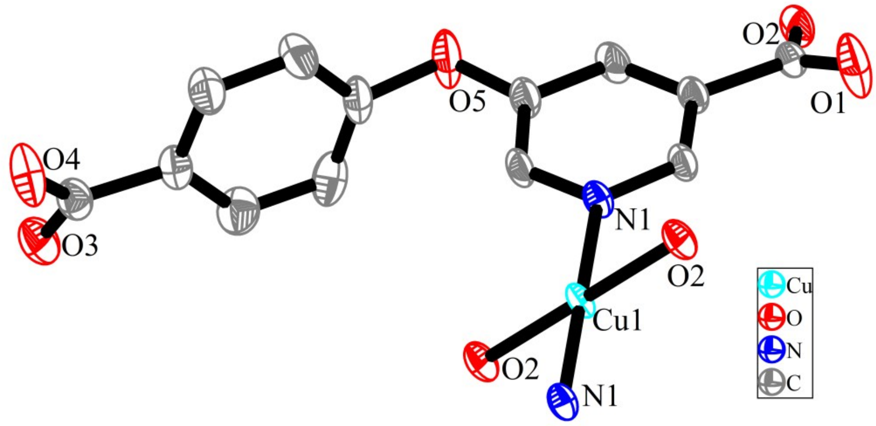

Fig. S3 The structural unit of **Cu1** with labeling scheme and 50% thermal ellipsoids (hydrogen atoms are omitted for clarity).

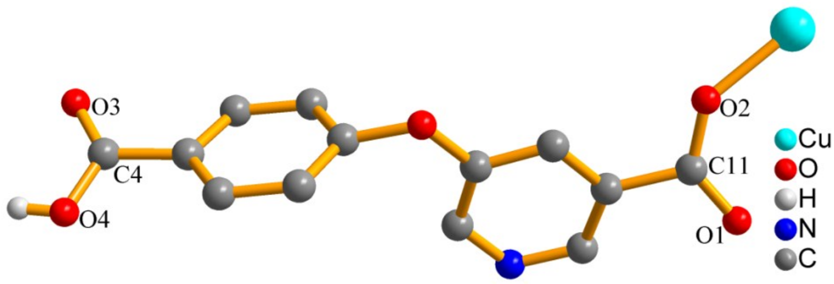

Fig. S4 Carboxyl coordination modes of **Cu1**.

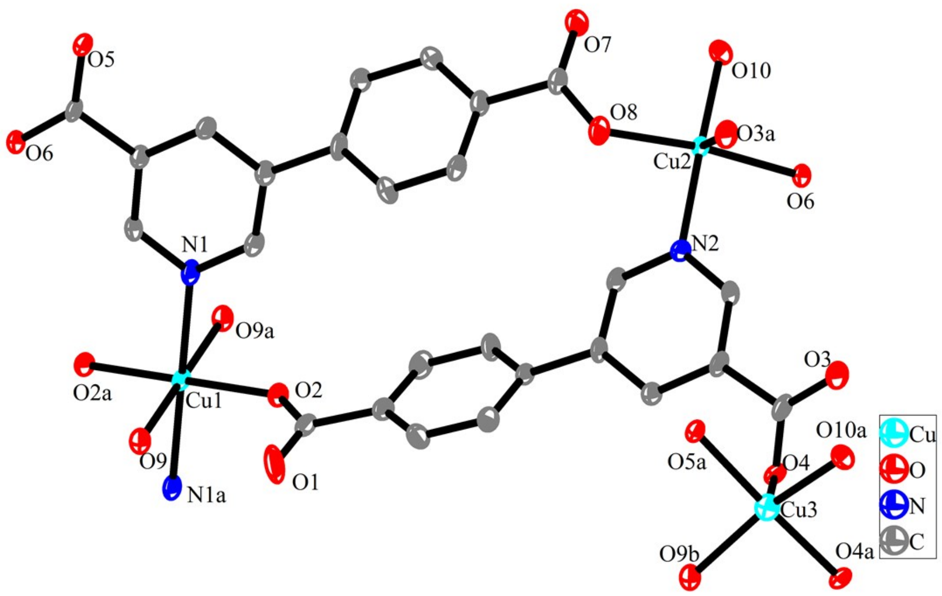

Fig. S5 The structural unit of **Cu2** with labeling scheme and 50% thermal ellipsoids (hydrogen atoms are omitted for clarity).

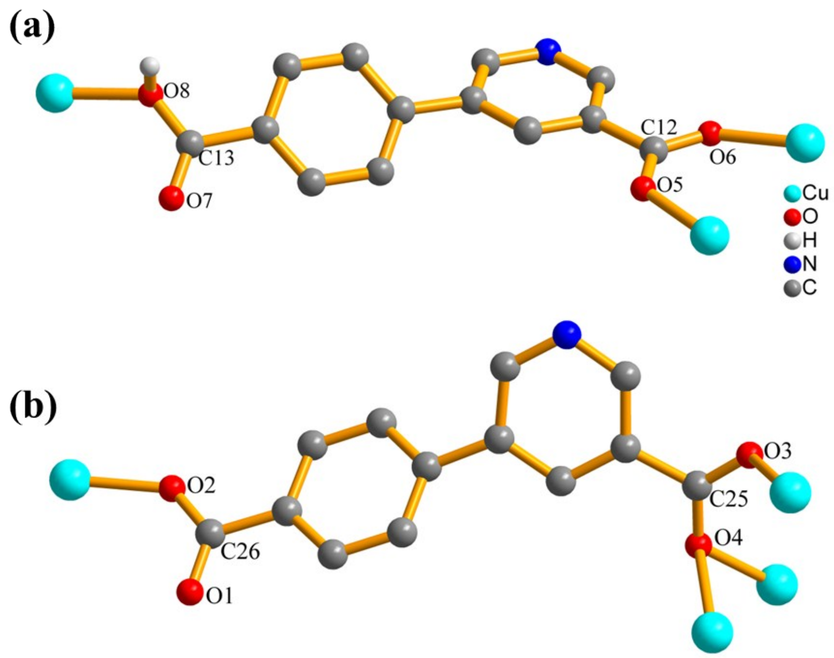

Fig. S6 Carboxyl coordination modes of **Cu2** (a) $HCPC^{-}$; (b) CPC^{2-}.

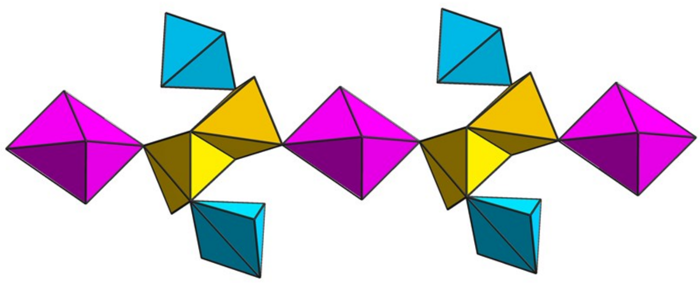

Fig. S7 Cu-O chain in **Cu2**

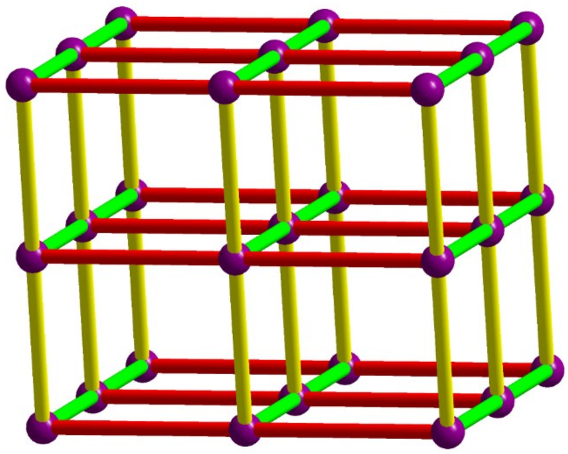

Fig. S8 Topological representation of 3D structure of **Cu2**.

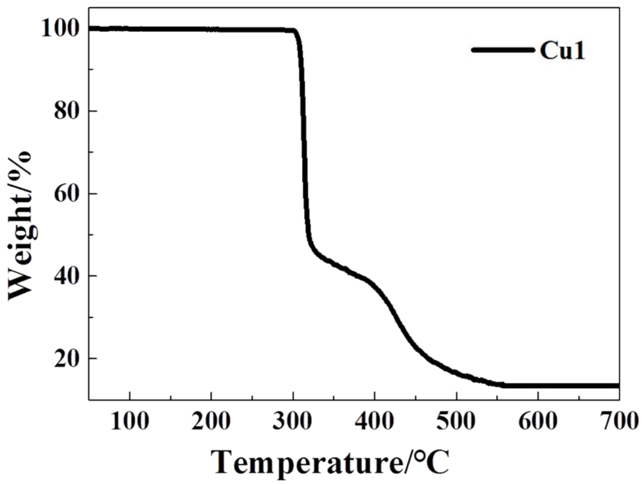

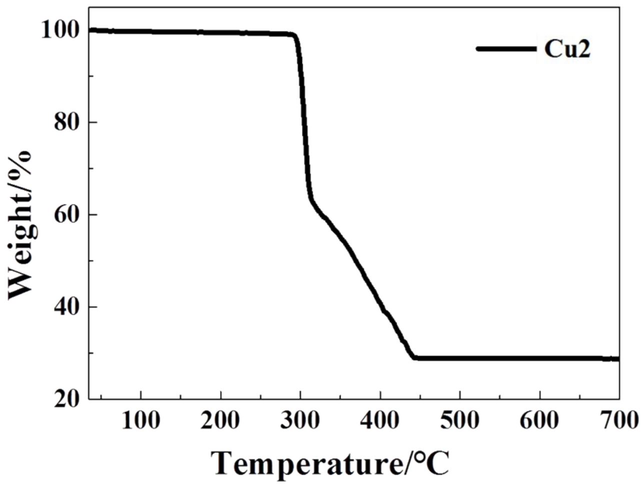

Fig. S9 Thermal gravimetric curves for **Cu1** and **Cu2**.

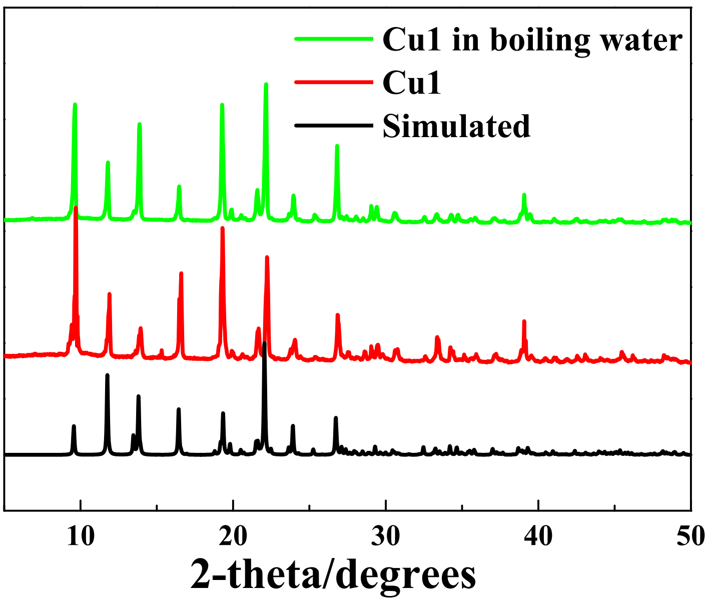

Fig. S10 PXRD patterns of **Cu1** with the relevant simulated pattern.

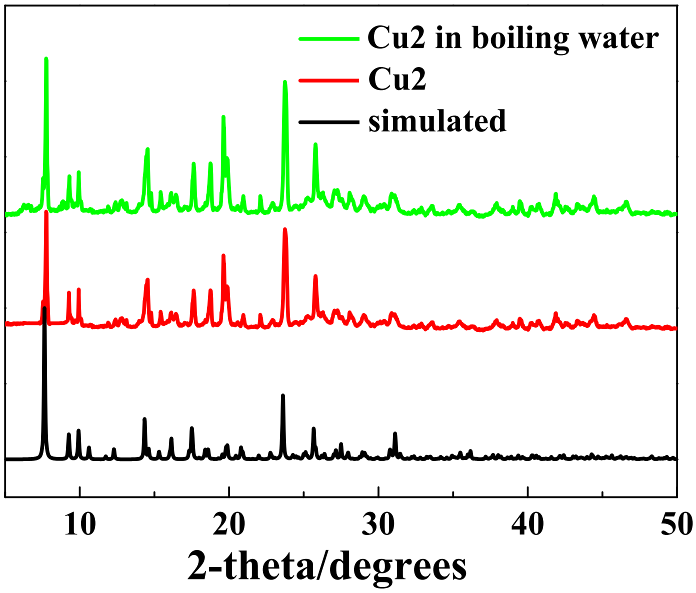

Fig. S11 PXRD patterns of **Cu2** with the relevant simulated pattern.

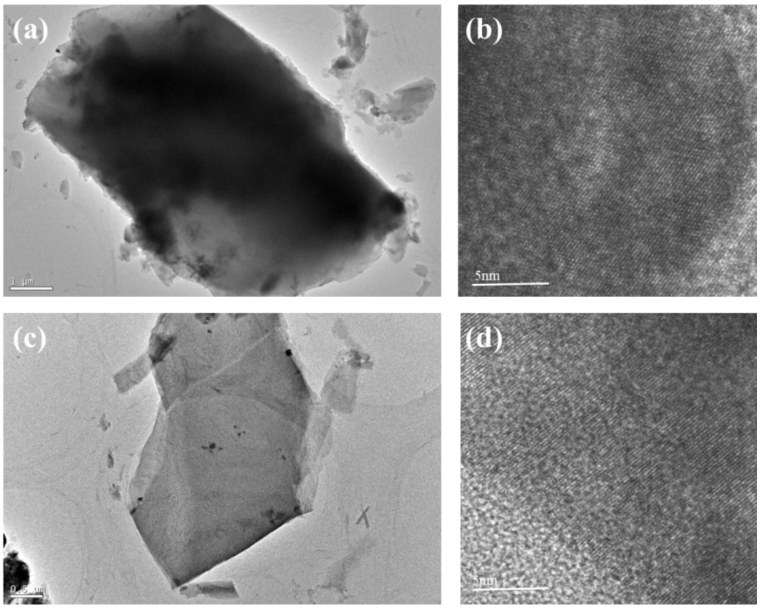

Fig. S12 TEM and HRTEM images of **Cu1** (a and b) and **Cu2** (c and d).

Table S2. Selected luminescent materials of Cu(II)-complexes.

No.	References	Complexes	Excitation(λ_{ex})	Emission(λ_{em})
1	*ChemPlusChem* 2016, 81, 857.	$[Cu_3(2\text{-eiba})_4(NO_3)_2]\cdot 5DMF$	370nm	445nm
2	*Cryst. Growth Des.* 2012, 12, 3786.	Cu-CPPs (CPP-1b)	358nm	396nm
3	*Cryst. Growth Des.* 2012, 12, 5025.	$\{[Cu(azim)_2(DMF)_2]\cdot(ClO_4)_2\cdot 2DMF\}_n$(**1**) $\{[Cu(azim)(Cl)\}_n$(**2**)	304nm 304nm	417nm 426nm
4	*Cryst. Growth Des.* 2013, 13, 3561.	[Cu(3-dppa)(1,3,5-HBTC)] (**1**) $[Cu(3\text{-dpha})(1,3,5\text{-HBTC})(H_2O)]\cdot H_2O$(**2**) $[Cu_3(3\text{-dpsea})(1,3,5\text{-BTC})_2(H_2O)_5]\cdot 4H_2O$(**3**) $[Cu(3\text{-dpba})(1,2\text{-BDC})]\cdot H_2O$(**4**) [Cu(3-dpha)(1,2-BDC)] (**5**) $[Cu(3\text{-dpsea})(1,2\text{-BDC})]H_2O$(**6**) $[Cu_2(3\text{-dpyp})(1,3\text{-BDC})_2(H_2O)4]\cdot 3H_2O$ (**7**) $[Cu(3\text{-dppa})(1,3\text{-BDC})(H_2O)]\cdot 2H_2O$ (**8**) $[Cu(3\text{-dppia})(1,3\text{-BDC})(H_2O)_2]\cdot 2H_2O$ (**9**) $[Cu_2(3\text{-dpsea})_2(1,3\text{-BDC})_2(H_2O)_2]\cdot 7H_2O$ (**10**) $[Cu(3\text{-dpba})(1,4\text{-NDC})]$ $3H_2O$(**11**) $[Cu(3\text{-dpyh})(1,4\text{-NDC})(H_2O)]\cdot 3H_2O$ (**12**)	320nm 320nm 320nm 320nm 320nm 320nm 320nm 320nm 320nm 320nm 320nm 320nm	399nm 400nm 400nm 399nm 404nm 396nm 420nm 399nm 398nm 396nm 399nm 397nm

		$[Cu(3\text{-}dpyh)_{0.5}(1,4\text{-}NDC)]\cdot H_2O$ (**13**)	320nm	384nm
5	*Cryst. Growth Des.* 2013, 13, 5050.	$[CuL(bbm)]\cdot 0.5H_2O$ (**1**) $[CuL(4,4'\text{-}bpy)_{0.5}]$ (**2**)	-- 280nm	-- 397nm
6	*CrystEngComm*, 2016, 18, 54.	$[Cu_2(\mu_2\text{-}L)_2(^{2,2'}BPy)_2(H_2O)_2](NO_3)_2\cdot S$ (**1**) $[Cu_2(\mu_2\text{-}L)_2(^{2,2'}BPy)_2(NO_3)_2]\cdot MeOH$ (**2**) $[Cu(L)(^{2,2'}BPy)_2]NO_3(H_2O)_2$ (**3**)	215nm 215nm 215nm	516nm 482nm 492nm
7	*Dalton Trans.*, 2013, 42, 8375.	$[Cu(3\text{-}dpye)(3\text{-}NPA)(H_2O)]\cdot 3H_2O$ (**1**) $[Cu(3\text{-}dpye)_{0.5}(5\text{-}AIP)(H_2O)]$(**2**) $[Cu(3\text{-}dpye)(1,3\text{-}BDC)]3H_2O$(**3**) $[Cu_3(3\text{-}dpye)(1,2\text{-}BDC)_2(\mu_2\text{-}OH)_2]$ (**4**) $[Cu_3(3\text{-}dpyb)(1,2\text{-}BDC)_2(\mu_2\text{-}OH)_2]$ (**5**) $[Cu(3\text{-}dpyh)_{0.5}(1,2\text{-}BDC)]\cdot H_2O$ (**6**) $[Cu(3\text{-}dpyh)_{0.5}(5\text{-}AIP)(H_2O)]$(**7**)	320nm 320nm 320nm 310nm 320nm 320nm 320nm	400nm 382nm 413nm 400nm 400nm 398nm 396nm
8	*Dalton Trans.*, 2013, 42, 5902.	$\{[Cu(bibim\text{-}4)_2(NO_3)](NO_3)\}_n$	240nm	305nm
9	*Inorg. Chem.* 2016, 55, 75.	$[(CH_3)_2NH_2]\cdot[Cu_2(CN)_3]$ (**1**) $[(CH_3)_2NH_2]\cdot[Cu_3(CN)_4]$ (**2**).	277nm --	540nm --
10	*Inorg. Chem. Front.*, 2015, 2, 373.	$[Cu(3\text{-}DPNA)(1,3,5\text{-}HBTC)]\cdot H_2O$ (**1**) $[Cu(4\text{-}DPNA)(1,3,5\text{-}BTC)_{2/3}]$(**2**)	320nm 320nm	465nm 411nm

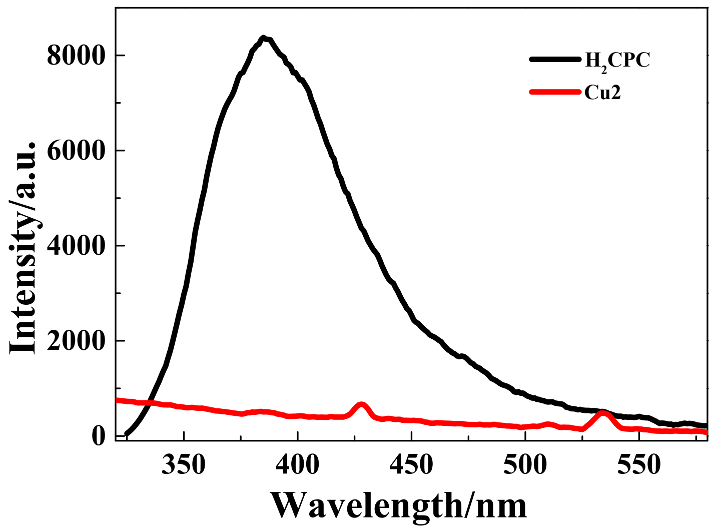

Fig. S13 Luminescence of H_2CPC and **Cu2** in aqueous solution.

Table S3. The ICP results of **Ln^{3+}@Cu1** and **Ln^{3+}@Cu2** (Ln^{3+} = Pr^{3+}, Nd^{3+}, Sm^{3+}, Eu^{3+}, Tb^{3+} and Dy^{3+}).

Samples	Cu^{2+}(wt%)	Ln^{3+}(wt%)
Cu1	10.95	––
Pr^{3+}@Cu1	9.42	13.84
Nd^{3+}@Cu1	9.39	14.12
Sm^{3+}@Cu1	9.34	14.64
Eu^{3+}@Cu1	9.32	14.77
Tb^{3+}@Cu1	9.26	15.34
Dy^{3+}@Cu1	9.23	15.64
Cu2	23.47	––
Pr^{3+}@Cu2	23.45	0.03
Nd^{3+}@Cu2	23.46	0.05
Sm^{3+}@Cu2	23.47	0.01
Eu^{3+}@Cu2	23.45	0.04
Tb^{3+}@Cu2	23.48	0.03
Dy^{3+}@Cu2	23.47	0.02

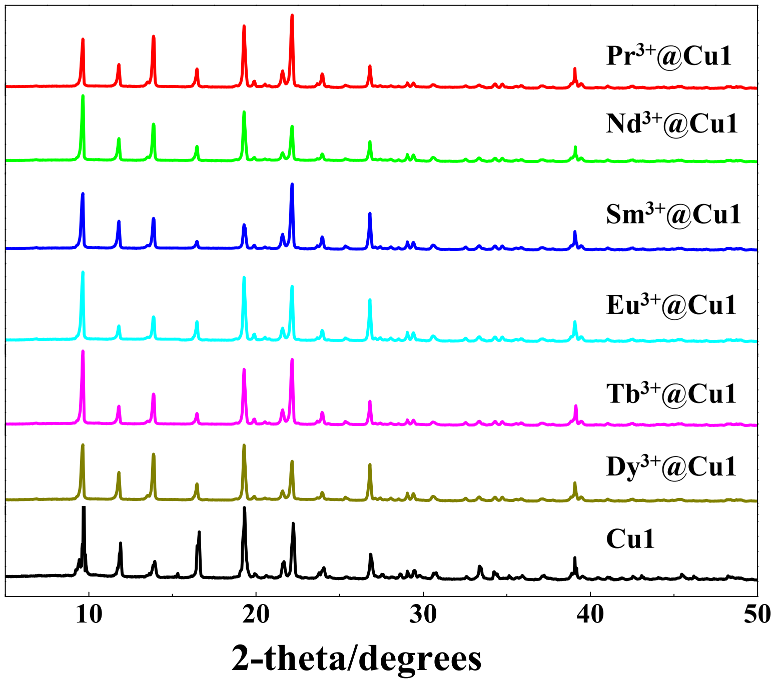

Fig. S14 PXRD patterns of **Ln^{3+}@Cu1** (Ln^{3+} = Pr^{3+}, Nd^{3+}, Sm^{3+}, Eu^{3+}, Tb^{3+} and Dy^{3+}) and **Cu1**.

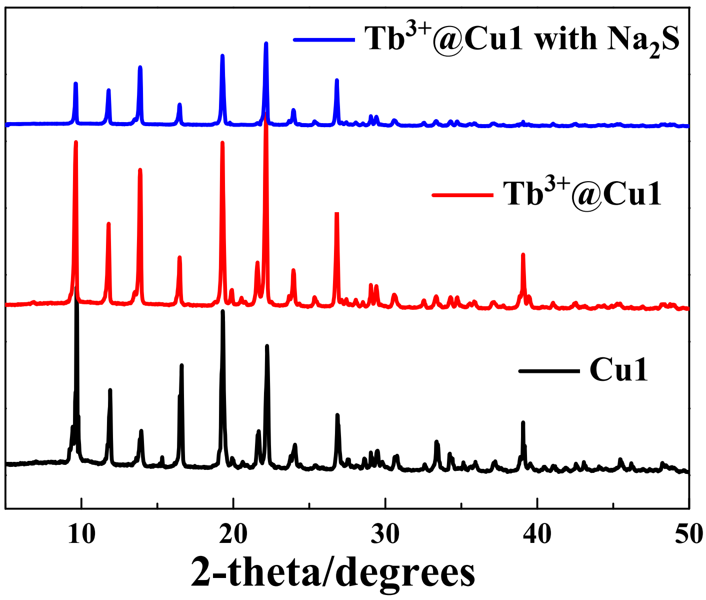

Fig. S15 PXRD patterns of **Tb^{3+}@Cu1** after the inclusion of Na_2S.

Table S4. The lifetime of MOFs **Cu1**, H_2CPOC, H_2CPC and **Tb^{3+}@Cu1**

Complex	τ_1 (μs)	A_1 (%)	τ_2 (μs)	A_2 (%)	χ^2	τ(μs)
Cu1	0.82	80.13	6.50	19.87	1.066	4.58
H_2CPOC	1.50	60.36	7.52	39.64	1.105	6.12
H_2CPC	0.55	39.56	6.31	60.44	1.021	6.00
Tb^{3+}@Cu1	259.10	100	--	--	1.143	259.10

Tb^{3+}@Cu1 **with Na_2S**	755.41	100	--	--	1.002	755.41

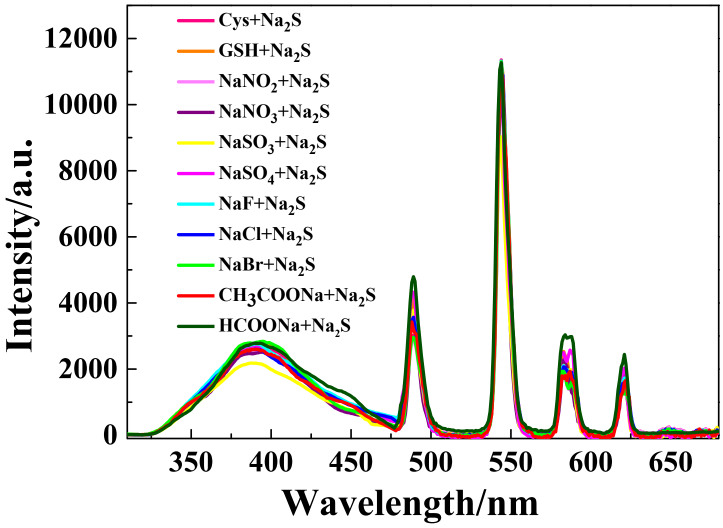

Fig. S16 Luminescence intensity of **Tb^{3+}@Cu1** with the interfering chemical species.

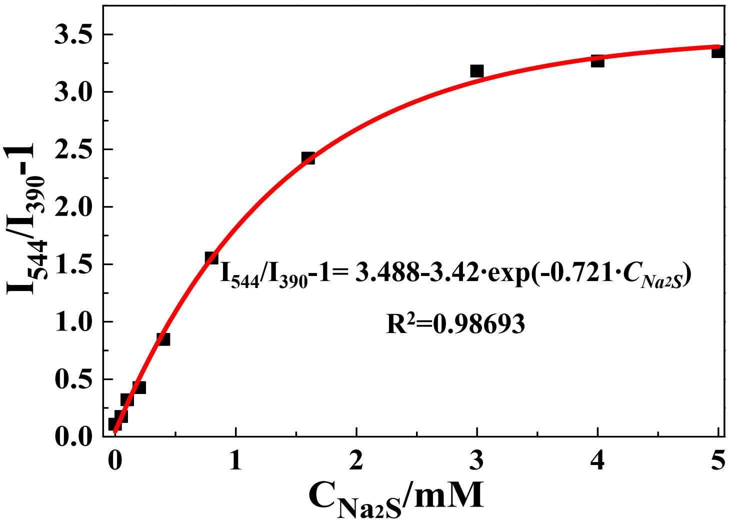

Fig. S17 Fitting curve between luminescence intensity ratio (I_{544}/I_{390}-1) and the concentrations (0-5 mM) of Na_2S.

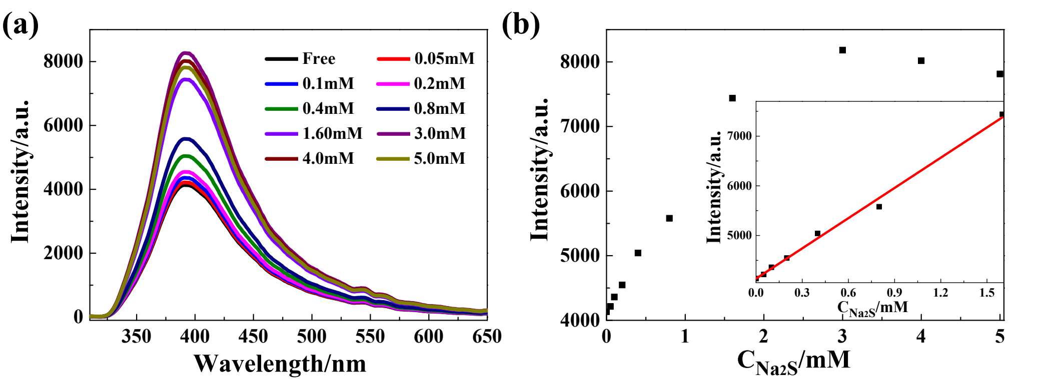

Fig. S18 (a) Luminescence spectra of **Cu1** with increasing concentrations (0-5 mM) of Na_2S; (b) Concentration dependence of the luminescence intensity I_{390} (0-5 mM) and Fitting curve between luminescence intensity I_{390} and the concentrations (0-1.6 mM) of Na_2S (insert).

Table S5. Standard deviation calculation and detection limit calculation.

No.	Luminescence intensity (I_{544}) of Tb^{3+}@Cu1	Luminescence intensity (I_{390}) of Tb^{3+}@Cu1	I_{544}/I_{390}-1	Luminescence intensity (I_{390}) of Cu1
1	2855.62 a.u.	3146.34 a.u.	0.101806	4129.21 a.u.
2	2840.23 a.u.	3125.89 a.u.	0.100576	4122.26 a.u.
3	2847.66 a.u.	3137.78 a.u.	0.101880	4139.02 a.u.
4	2839.77 a.u.	3128.23 a.u.	0.101579	4118.25 a.u.
5	2852.39 a.u.	3143.56 a.u.	0.102079	4136.53 a.u.
Standard Deviation (σ)	--	--	0.000591	8.92
Slope (*S*)	--	--	1.479 mM^{-1}	2018.59 mM^{-1}
Detection limit (3σ/*S*)	--	--	1.20 μM	13.25 μM

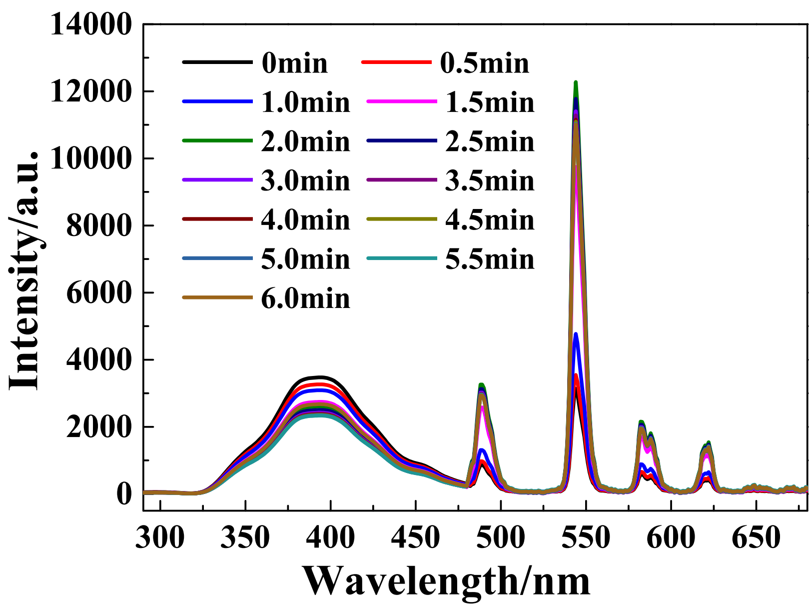

Fig. S19 Luminescence intensity of **Tb^{3+}@Cu1** towards addition of Na_2S (5 mM) after 0-6 min.

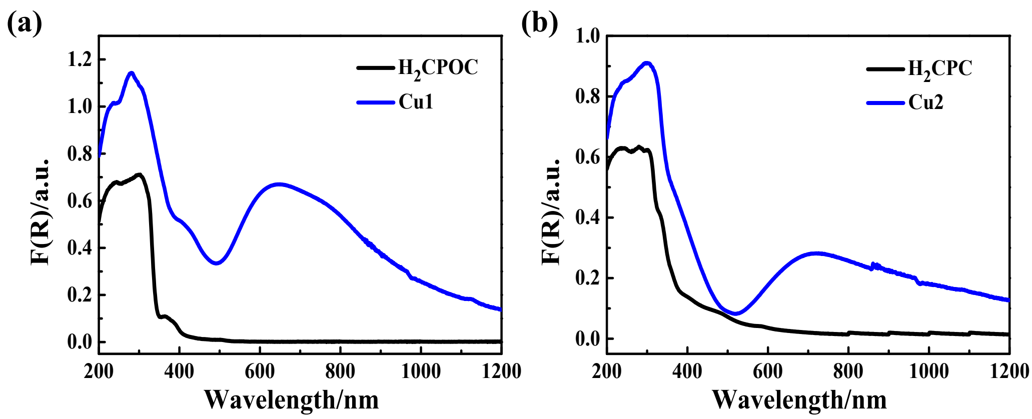

Fig. S20 Plots of the UV-vis absorption spectra of (a) H_2CPOC and **Cu1**; (b) H_2CPC and **Cu2** at room temperature.

Table S6. Selected luminescent materials for sensing H_2S.

No.	probes	solution	response time	detection limit	references
1	SFP-1	Live cells	60 min	5-10 μM	*Nat. Commun.*2011, 2, 495
	SFP-2		60 min	5-10 μM	
2	cpGFP-Tyr66pAzF	Live cells	15 min	10 μM	*J. Am. Chem.Soc*. 2012, 134, 9589
3	FSI	Live cells	120 min	5-10 μM	*Chem. Commun*. 2012, 48, 8395.
4	Sensor 4	Live cells	30 min	10 μM	*Biomaterials*, 2013, 34, 7429.
5	CLSS-2	PIPES buffer	60 min	4.6 ± 2.0 μM	*J. Am. Chem. Soc*. 2013, 135, 16697.
6	AMP/Tb/Ag	HEPES buffer	2 min	0.8 μM	*Anal. Chem*. 2013, 85, 11020.
7	Zr-UiO-66-N_3	Live cells	3 min	118 μM	*Sci. Rep*. 2014, 4, 7053.
8	Zr-UiO-66-NO_2	HEPES buffer	7.7 min	188 μM	*Chem. Eur. J.* 2015, 21, 9994.
9	IRMOF-3-N3	HEPES buffer	2 min	28.3 μM	*Appl. Surf. Sci*. 2015, 355, 814
10	Ce-UiO-66-N_3	HEPES buffer	12.7 min	12.2 μM	*CrystEngComm,* 2016, 18, 4374.
	Ce-UiO-66-NO_2		12.7 min	34.84 μM	
11	GMP/Tb/OX–Cu	HEPES buffer	3 min	0.5 μM	*Anal. Methods*, 2017, 9, 1004.
12	**Cu1**	HEPES buffer	--	13.25 μM	This work
	Tb^{3+}@Cu1		< 2 min	1.20 μM	